[Electronic Supplementary Information]

Multifunctional chiral cationic porous organic polymers: gas uptake and heterogeneous asymmetric organocatalysis

Zhenwei Zhang,‡[a] Xiaochen Shen,‡[a] Ziping Li,[a] Si Ma,[a] Hong Xia,[b] and Xiaoming Liu*[a]

[a]*College of Chemistry, Jilin University, Changchun, 130012, P.R. China.*
[b]*State Key Laboratory on Integrated Optoelectronics, College of Electronic Science and Technology, Jilin University, Changchun 130012, P.R. China.*

Email: xm_liu@jlu.edu.cn

Table of Content

Section 1. General Information

The preparation of monomers and the design of porous organic polymers for synthesis are based on previous reports and our previous work.[1] FT-IR spectra were recorded from 400 to 4000 cm^{-1} on an Avatar FT-IR 360 spectrometer by using KBr pellets. ^{1}H and ^{13}C NMR spectra were measured in $CDCl_3$ on Bruker-Avance with TMS as an internal reference. Solid-state ^{13}C CP/MAS NMR measurement was recorded using a Bruker AVANCE III 400 WB spectrometer at a MAS rate of 5 kHz and a CP contact time of 2 ms. Powder X-ray diffraction data were recorded on a PANalytical BV Empyrean diffractometer by depositing powder on glass substrate, from $2\theta = 1.5°$ to 30° with 0.02° increment at 25 °C. Field emission scanning electron microscopy was performed on a SU8020 model HITACHI microscope. X-ray photoelectron spectroscopy (XPS) was performed using an ESCALAB 250 spectrometer. Powder X-ray diffraction data were recorded on a PANalytical B.V. Empyrean diffractometer by depositing powder on glass substrate. Thermogravimetric analysis (TGA) was performed on a TGA Q500 thermogravimeter by measuring the weight loss under nitrogen. Nitrogen sorption isotherms were measured at 77 K with a JW-BK 132F analyzer. Before measurement, the samples were degassed in vacuum at 120 ^{o}C for more than 10 h. The Brunauer-Emmett-Teller (BET) method was utilized to calculate the specific surface areas and pore volume, the Saito-Flory method was applied for the estimation of pore size distribution. Enantiomeric excesses of products were determined by chiral HPLC by using Daicel Chiralpak OD-H columns with a UV detector set at 254 nm. Charge and chiral properties are characterized by Zetasizer Nan ZS90 and CD spectra (PMS 450), respectively.

Section 2. Syntheses of Monomers and Polymers

Synthesis of monomer CC-NSA$_H$@Br (J. Am. Chem. Soc., 2003, 125, 5139): A mixture of 4,5-dihydro-3H-dinaphtho [2,1-c:1',2'-e] azepine (148 mg, 0.5 mmol), 2,2'-bis(bromomethyl)-1,1'-binaphthyl (242 mg, 0.55 mmol) and K_2CO_3 (104 mg, 0.75 mmol) in dry acetonitrile (5 mL) was heated to reflux, and stirring was maintained for 10 h. The resulting mixture was poured into water and extracted with CH_2Cl_2. The organic extracts were dried over Na_2SO_4 and concentrated. The residue was purified by column chromatography on silica gel (MeOH/CH_2Cl_2 = 1:30) to furnish CC-NSA$_H$@Br (184 mg, 0.28 mmol, 56% yield). ^{1}H NMR (400 MHz, $CDCl_3$): δ 8.38 (4H, d, *J* = 8.4 Hz, Ar-H), 8.17 (4H, d, *J* = 8.4 Hz, Ar-H), 8.10 (4H, d, *J* = 8.4 Hz, Ar-H), 7.62 (4H, ddd, *J* = 8.4, 6.6, 1.4 Hz, Ar-H), 7.26-7.44 (8H, m, Ar-H), 4.52 (4H, d, *J* = 13.2 Hz, Ar-CH_2), 3.92 (4H, d, *J* = 13.2 Hz, Ar-CH_2) ppm; ^{13}C NMR (100 MHz, $CDCl_3$): δ 136.5, 134.5, 131.3, 131.1, 128.7, 127.7, 127.7, 127.4, 127.2, 125.2, 60.9 ppm.

Synthesis of monomer CC-NSA$_{Ph}$@Br: CC-NSA$_{Ph}$@Br was prepared in a similar manner as described for CC-NSA$_H$@Br. (90% yield). ^{1}H NMR (400 MHz, $CDCl_3$): δ 8.34 (2H, s, Ar-H), 8.11 (2H, d, *J* = 8.4 Hz, Ar-H), 7.84 (2H, d, *J* = 8.4 Hz, Ar-H), 7.74 (2H, br, Ph), 7.63 (2H, ddd, *J* = 8.0, 7.2, 1.2 Hz, Ar-H), 7.49 (2H, ddd, *J* = 8.0, 7.2, 1.2 Hz, Ar-H), 7.31-7.36 (4H, m, Ar-H), 7.09-7.22 (6H, m, Ar-H), 7.20-8.20 (8H, br, Ph), 6.32 (2H, d, *J* = 8.4 Hz, Ar-H), 5.01 (2H, d, *J* = 14.0 Hz, Ar-CH_2), 4.40 (2H, d, *J* = 13.6 Hz, Ar-CH_2), 4.24 (2H, d, *J* = 13.2 Hz, Ar-CH_2), 3.71 (2H, d, *J* = 13.2 Hz, Ar-CH_2) ppm; ^{13}C NMR (100 MHz, $CDCl_3$): δ 139.1, 139.0, 136.1, 133.8, 113.8, 132.6, 130.9, 130.8, 130.0, 129.9, 128.6, 128.4, 128.2, 128.1, 127.4, 124.3, 127.2, 126.8, 126.6, 124.7, 122.3, 62.3, 57.5 ppm.

Synthesis of monomer CC-NSA$_{Naph}$@Br: CC-NSA$_{Naph}$@Br was prepared in a similar manner as described for CC-NSA$_H$@Br. (76% yield). ^{1}H NMR (400 MHz, $CDCl_3$): δ 8.47 (s, 3H, Ar-H), 8.13 (d, 5H, *J* = 8.0 Hz, Ar-H), 7.77 (t, 4H, *J* = 12.0 Hz, Np), 7.64 (t, 4H, *J* = 16.0 Hz, Ar-H), 7.31-7.40 (m, 8H, Np), 7.18 (d, 2H, *J* = 8.0 Hz, Ar-H), 7.07 (t, 2H, *J* = 16.0 Hz, Ar-H), 6.93 (d, 2H, *J* = 8.0 Hz, Ar-H), 6.01 (br, 4H, Np), 5.01 (br, 2H, Ar-CH_2),

4.42 (d, 2H, *J* = 16.0 Hz, Ar-CH_2), 4.15 (d, 2H, *J* = 12.0 Hz, Ar-CH_2), 3.60 (d, 2H, *J* = 12.0 Hz, Ar-CH_2) ppm; ^{13}C NMR (100 MHz, $CDCl_3$): δ 139.7, 139.6, 136.2, 134.3, 134.0, 133.5, 133.1, 131.0, 129.1, 128.9, 128.8, 128.7, 128.6, 128.3, 128.1,127.9, 127.8, 127.7, 127.6, 127.5, 127.1, 126.9, 125.0, 123.1, 62.5, 57.8 ppm.

Synthesis of CC-NSA$_{Ph}$-HCP@Br. To the mixture of monomer CC-NSA$_{Ph}$@Br (48.3 mg, 0.06 mmol) and anhydrous $FeCl_3$ (77.9 mg, 0.48 mmol) in 1,2-dichloroethane (2.0 mL), FDA (42.5 μL, 0.48 mmol) was added at room temperature. The mixture was heated to 80 ^{o}C and stirred for 24 h under a nitrogen atmosphere. The mixture was then cooled to room temperature, the precipitated network was filtered and washed with dichloromethane, methanol, and tetrahydrofuran, respectively. The product was then dispersed in 5 mL 1:1 H_2O/methanol saturated solution of sodium bromide. After the mixture was stirred for 24 h at room temperature, the residue was filtered. Repeated the above step three times, the precipitate was washed with plenty of water. The further purification of the network was carried out by Soxhlet extraction from methanol and tetrahydrofuran for 24 h, respectively. The product was dried in vacuum for 24 h at 80 ^{o}C to give a brown powder 53.2 mg.

Synthesis of CC-NSA$_{Naph}$-HCP@Br. To the mixture of monomer CC-NSA$_{Naph}$@Br (55.0 mg, 0.06 mmol) and anhydrous $FeCl_3$ (77.9 mg, 0.48 mmol) in 1,2-dichloroethane (2.0 mL), FDA (42.5 μL, 0.48 mmol) was added at room temperature. The mixture was heated to 80 ^{o}C and stirred for 24 h under a nitrogen atmosphere. The mixture was then cooled to room temperature, the precipitated network was filtered and washed with dichloromethane, methanol, and tetrahydrofuran, respectively. The product was then dispersed in 5 mL 1:1 H_2O/methanol saturated solution of sodium bromide. After the mixture was stirred for 24 h at room temperature, the residue was filtered. Repeated the above step three times, the precipitate was washed with plenty of water. The further purification of the network was carried out by Soxhlet extraction from methanol and tetrahydrofuran for 24 h, respectively. The product was dried in vacuum for 24 h at 80 ^{o}C to give a brown powder 59.1 mg.

Section 3. Solid State ^{13}C CP/MAS NMR

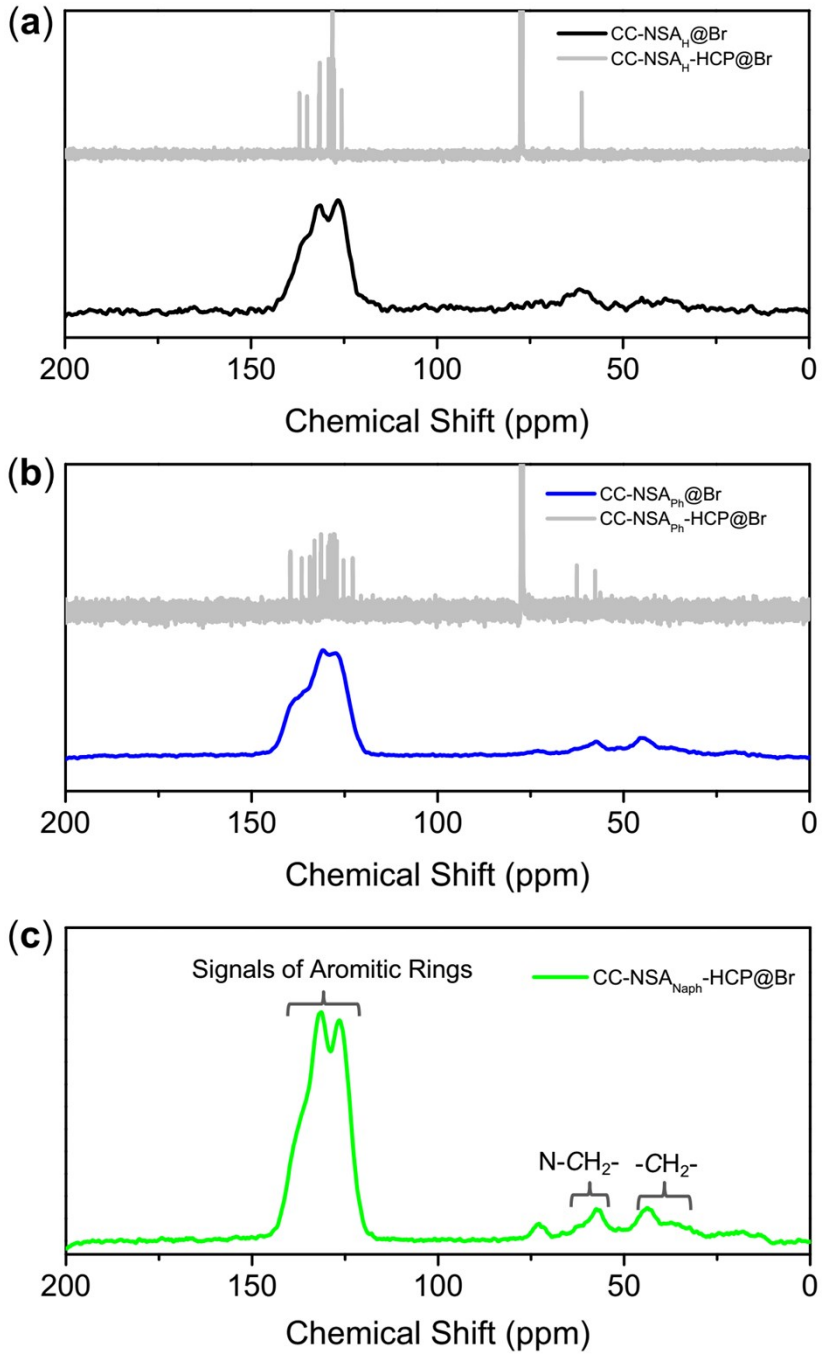

Figure S1. The solid-state ^{13}C-CP/MAS NMR spectra of chiral cationic polymers (CC-NSA$_R$-HCPs@Br) and ^{13}C-NMR spectra of chiral N-spiroammonium salt monomers (CC-NSA$_H$@Br and CC-NSA$_{Ph}$@Br) in $CDCl_3$. The signals from 120 to 145 ppm are assignable to aromatic carbon, and the weak peaks at about 58 and 42 ppm are attributed to the two types of methylene carbon in the polymer networks.

Section 4. IR Spectra

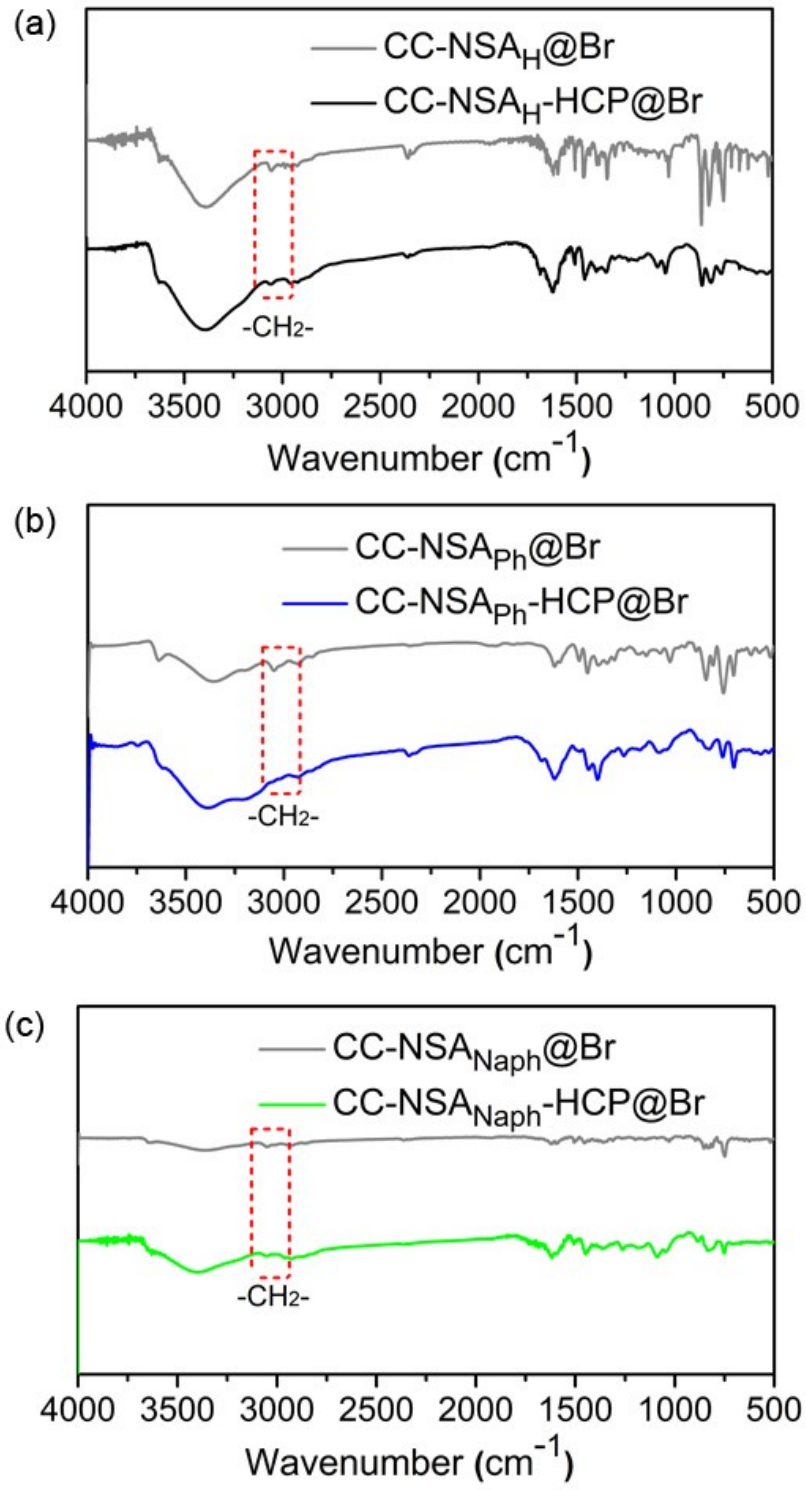

Figure S2. FT-IR spectra of chiral N-spiroammonium salt monomers (CC-NSA$_R$@Br) and polymers (CC-NSA$_R$-HCPs@Br). The peaks at around 2932 cm^{-1} are originating from C-H stretching vibrations of –CH_2– groups.

Section 5. PXRD Spectra

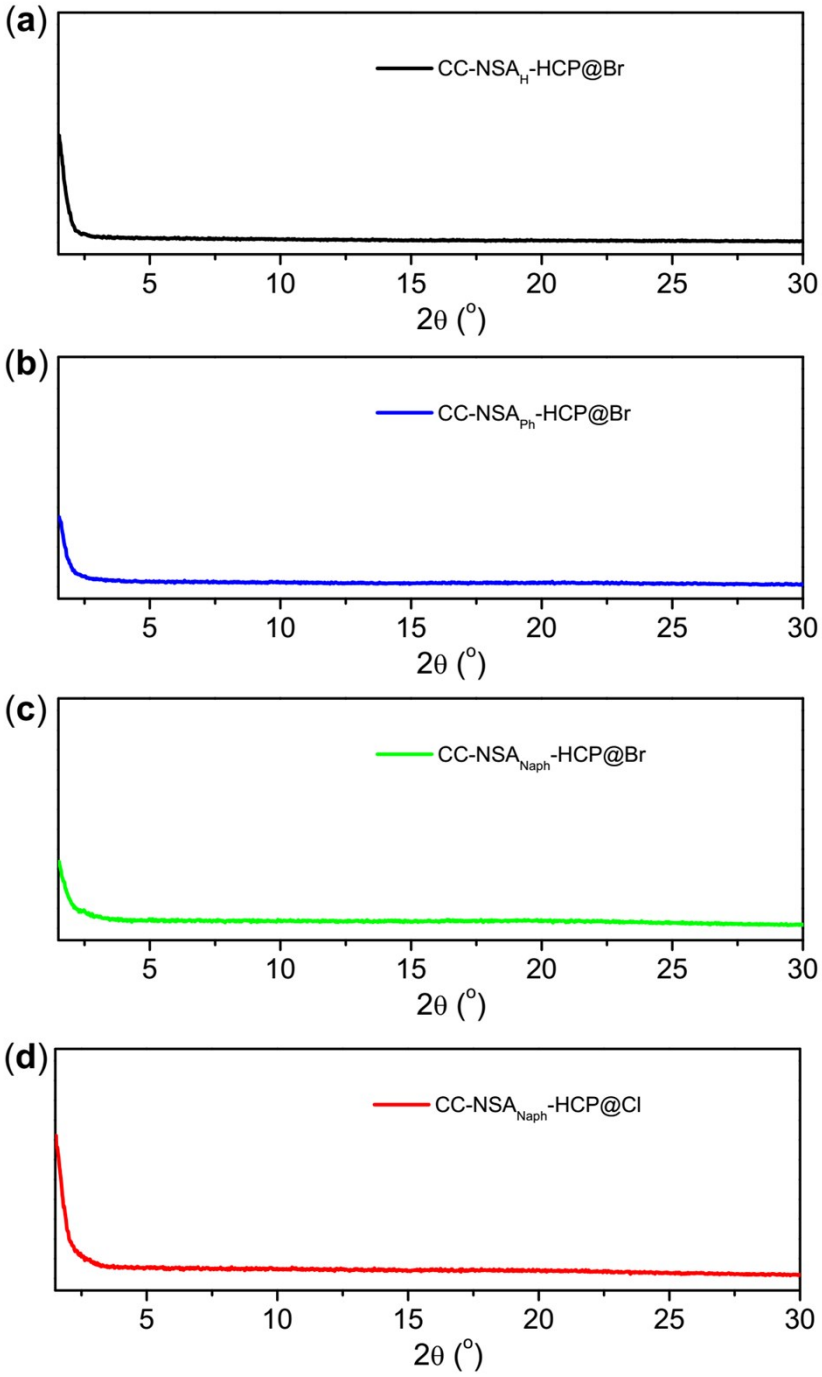

Figure S3. PXRD curves of the polymer CC-NSA$_R$-HCPs@X.

Section 6. SEM Images

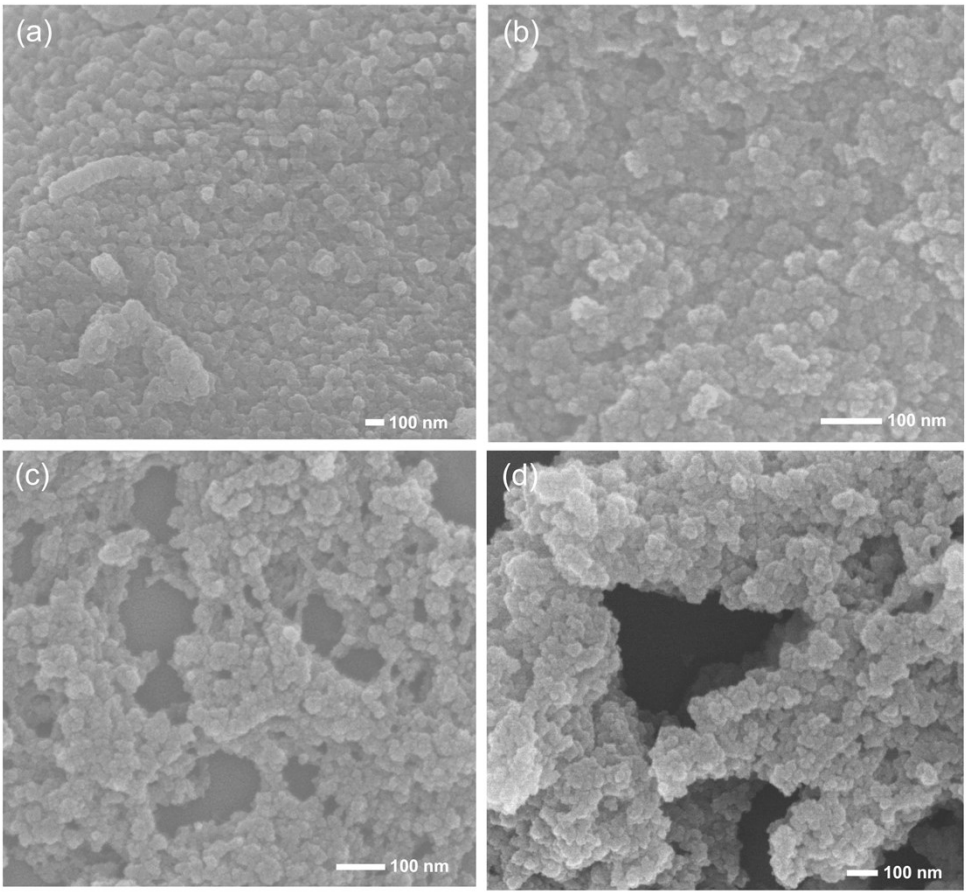

Figure S4. SEM images of the chiral cationic polymer networks: (a) CC-NSA_H-HCP@Br (b) CC-NSA_{Ph}-HCP@Br (c) CC-NSA_{Naph}-HCP@Br (d) CC-NSA_{Naph}-HCP@Cl.

Section 7. TGA Curves

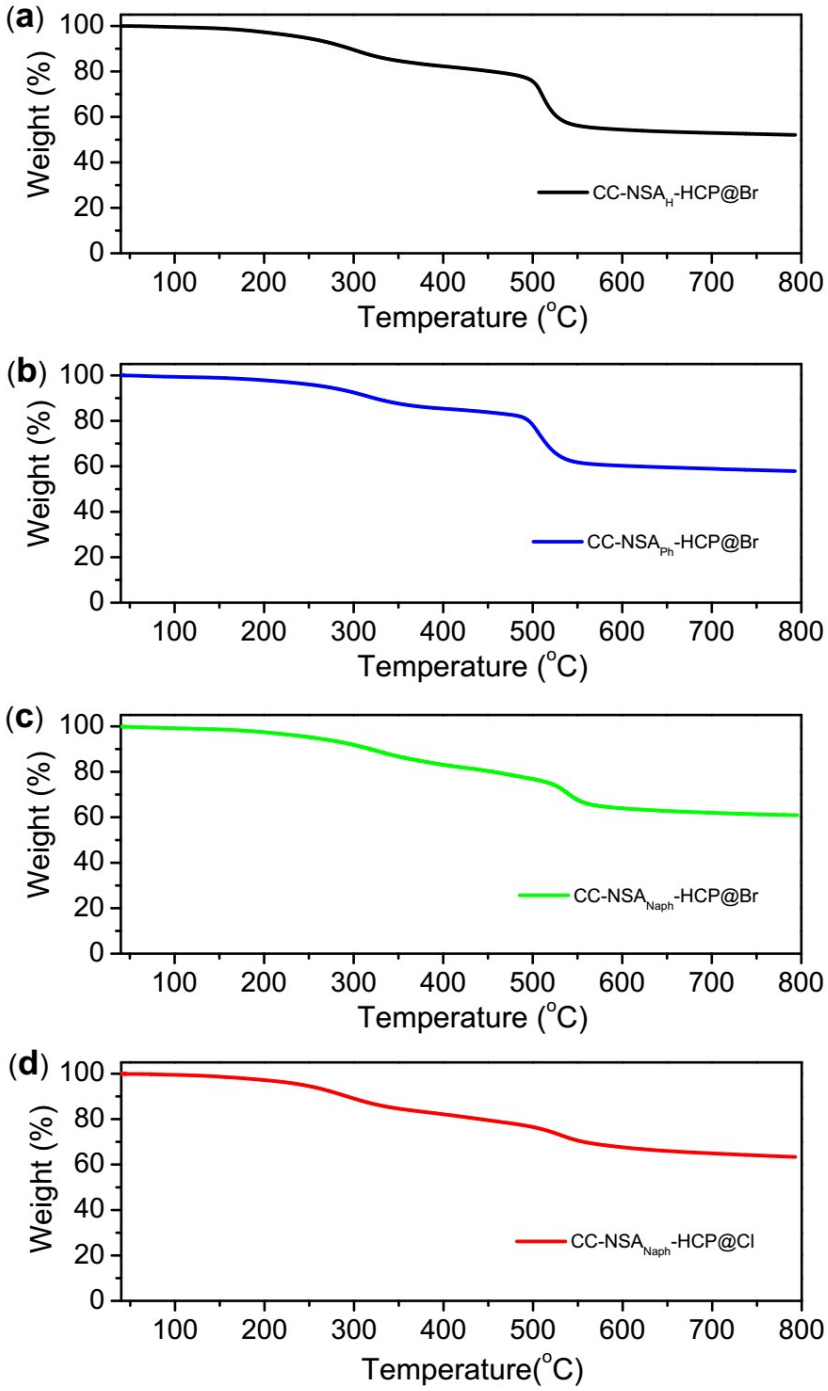

Figure S5. TGA curves of the polymer CC-NSA$_R$-HCPs@X

.

Section 8. XPS Spectra

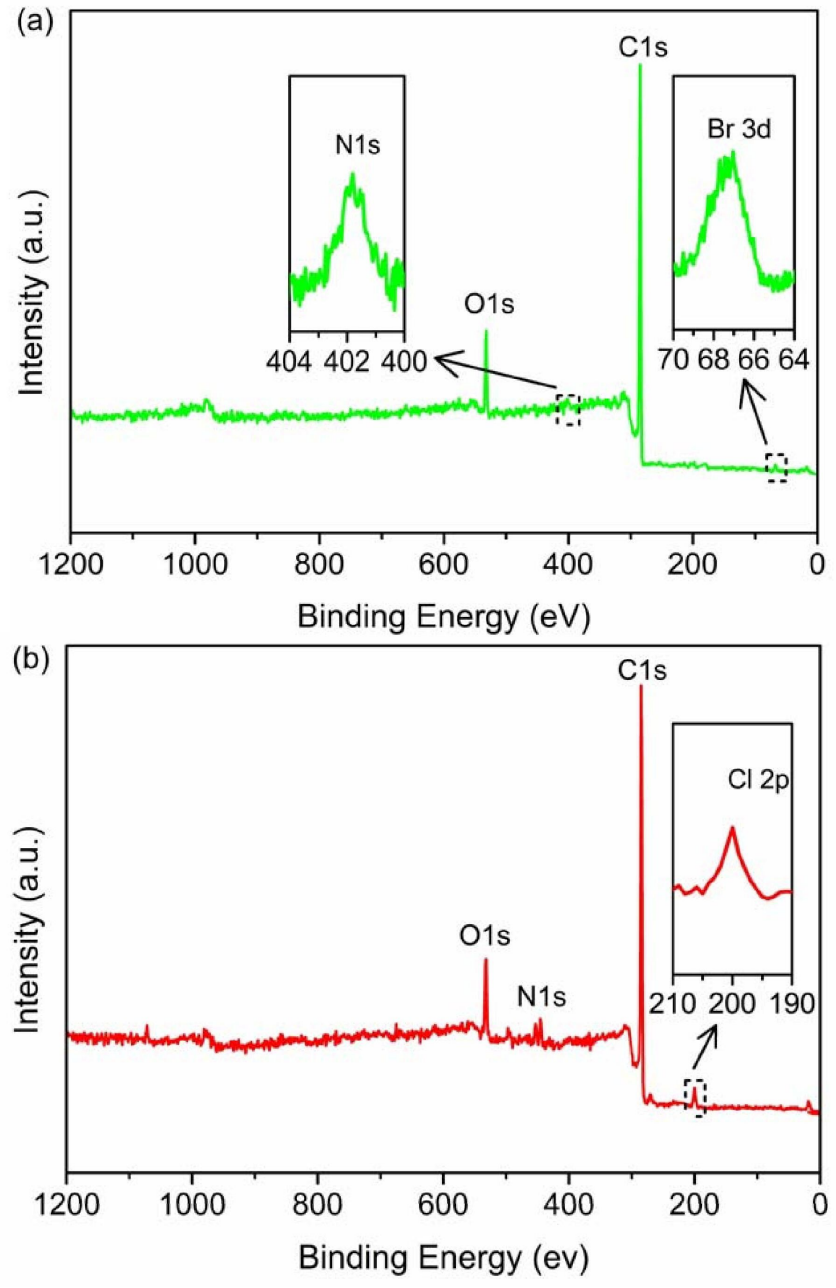

Figure S6. XPS patters of CC-NSA$_{Naph}$-HCPs@X recorded from 0 to 1200 eV: (a) CC-NSA$_{Naph}$-HCP@Br; (b) CC-NSA$_{Naph}$-HCP@Cl.

Section 9. CD spectra

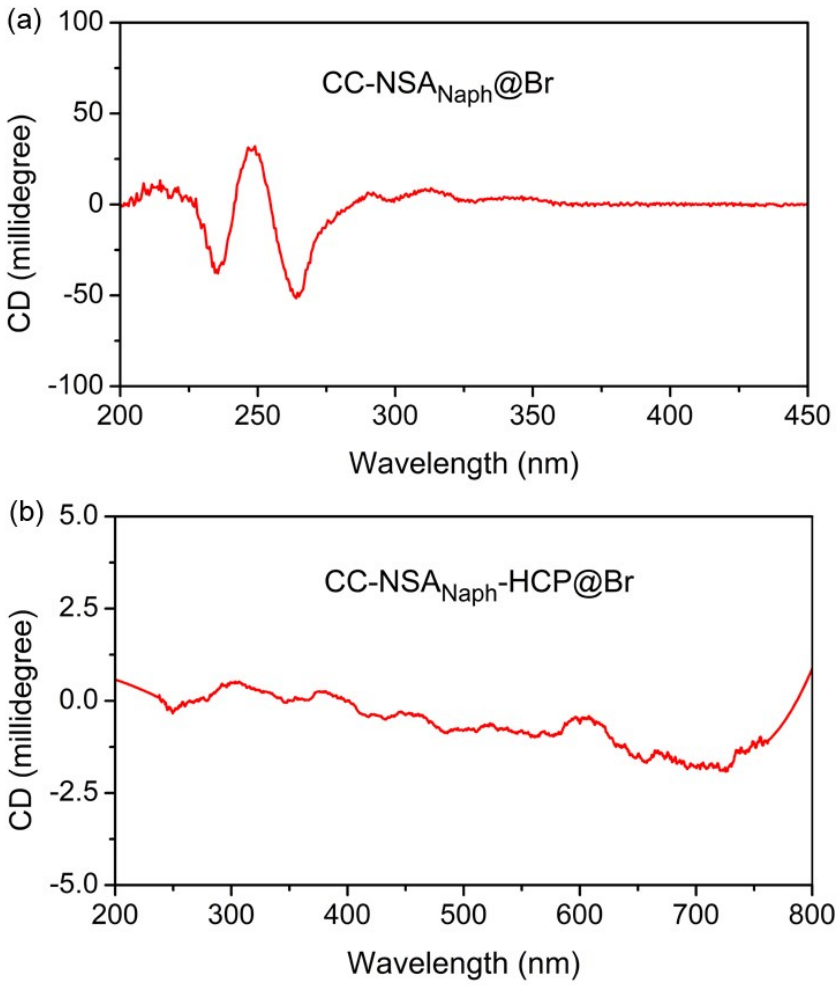

Figure S7. CD spectra of (a) CC-NSA$_{Naph}$@Br and (b) CC-NSA$_{Naph}$-HCP@Br.

Section 10. Zeta Potential Distribution

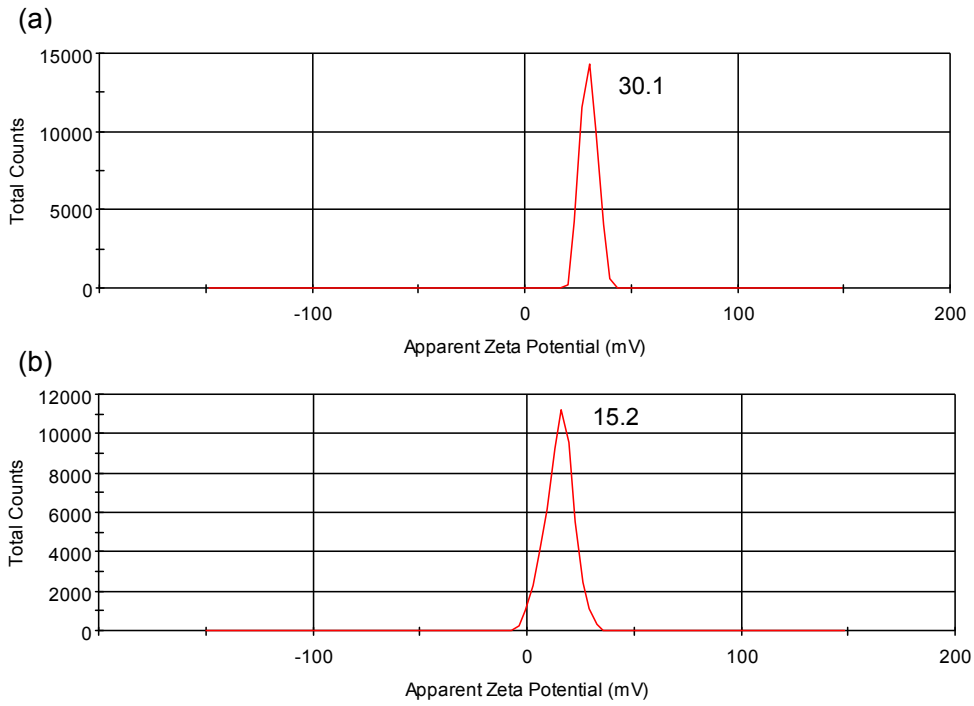

Figure S8. Zeta Potential Distribution of (a) CC-NSA$_{Naph}$-HCP@Br and (b) CC-NSA$_{Naph}$@Br.

Section 11. Porosity Parameters and Gas Uptakes

Table S1. Summary of porosity parameters and gas uptakes for CC-NSA$_R$-HCPs@X.

Polymers		CC-NSA$_H$-HCP@Br	CC-NSA$_{Ph}$-HCP@Br	CC-NSA$_{Naph}$-HCP@Br	CC-NSA$_{Naph}$-HCP@Cl
SA_{BET} (m^2 g^{-1})		549	722	788	724
SA_L (m^2 g^{-1})		623	817	844	808
Pore Vol. (cm^3 g^{-1})		0.422	0.618	0.569	0.571
Microporous Vol. (cm^{3}g^{-1})		0.215	0.292	0.309	0.286
Pore Size (nm)		1.05	0.64	0.99	0.95
H_2 Uptake (mg g^{-1})	87K/1bar	2.13	4.34	3.13	2.25
	77K/1bar	2.98	6.16	4.09	3.39
Q_{st} (KJ mol^{-1})		6.6	7.0	6.3	5.9

Section 12. Summary and comparison of hydrogen storage capacity

Table S2. A summary for the H_2 storage performance of CC-NSA_{Ph}-HCP@Br and other POPs reported.

POPs[a]	SA_{BET} ($m^2\ g^{-1}$)	Pore Vol. ($cm^3\ g^{-1}$)	Microporous Vol. ($cm^3\ g^{-1}$)	Pore Size (nm)	H_2 Uptake	Ref.
PPOP-1	720	0.36	0.18	0.59	1.14	23a
PPOP-2	920	0.41	0.21		1.08	
PPOP-3	880	0.41	0.20		1.28	
hPOP-3	350	0.27	0.07	0.58/1.75	1.28	23b
hPOP-4	1060	0.93	0.26	0.50/0.58	1.90	
hPOP-5	1300	1.12	0.28	0.59	2.17	
hPOP-6	1320	1.40	0.21	0.59	1.67	
Azo-1	571	1.342	0.156	3.47	0.86	23c
Azo-2	675	1.686	0.186	2.72	1.15	
Azo-3	520	1.383	0.164	2.89	0.97	
BLP-1(Cl)	1364	0.746	-	1.3	1.10	23d
BLP-1(Br)	503	0.303			0.68	
BLP-2(Cl)	1174	0.649			1.30	
BLP-2(Br)	849	0.571			0.98	
PCTF-1	2235	1.56	0.79	2-6	1.86	23e
PCTF-2	784	0.76	0.29	2-10	0.90	
TPE-CMP	854	0.57	-	1.08	1.5	23f
MPOP-1	718	0.54	0.11	0.7-1.5	0.88	23g
MPOP-2	790	1.07	0.11		1.0	
MPOP-3	1026	0.77	0.16		0.96	
PDMTPAS[c]	808	0.70	0.21	1.0/1.8	5.00	23h
PDPTPAS[c]	666	0.65	0.17		5.26	
PDMCzS[c]	1137	0.89	0.41		7.46	
CPOP-16	780	0.59	-	0.59	1.44	23i
CPOP-17	770	0.48		0.59	1.63	
CPOP-18	1040	0.77		0.52	2.29	
CPOP-19	1130	0.80		0.59	2.39	
FCBCz	1067	0.71	0.43	0.89/1.54	1.56	23j
FCTCz	1845	2.91	0.51	0.98/1.58	1.94	
CO-PP-0[d]	695	0.857	0.264	1.3/2.6	1.3	23k
SBLeCOePP-7[d]	820	0.932	0.355	1.2/3.0	1.6	
SBLeCOePP-20[d]	1421	0.857	0.616	0.8/1.5	2.2	
SBLeCOePP-C-7[d]	2679	1.335	1.150	0.8/2.6	4.4	
SBLeCOePP-C-20[d]	2330	1.270	0.780	1.9	4.1	
CC-NSA_{Ph}-HCP@Br[e]	722	0.618	0.292	0.64	6.16	Our

[a]Hydrogen gravimetric uptake capacities (wt %) at 77 K measured at hydrogen equilibrium pressure of 1.0 bar;

[b]Calculated from N2 adsoption data collected at 77 K applying the Langmuir model except where indicated; [c]Data obtained at 77.3 K and 1.13 bar (mmol g^{-1}); [d]Hydrogen gravimetric uptake capacities (wt %) at 77 K measured at hydrogen equilibrium pressure of 20 bar; [e]Hydrogen gravimetric uptake capacities (mg g^{-1}) at 77 K measured at hydrogen equilibrium pressure of 1 bar.

Section 13. Characterization Data of Catalytic Products

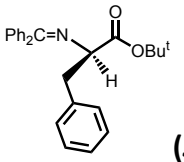

(*S*)-*tert*-butyl-N-(diphenylmethylene)-phenylalaninate (3a): ^{1}H NMR (400 MHz, $CDCl_3$) δ: 7.57-7.59 (2H, m, Ph), 7.26-7.36 (6H, m, Ph), 7.14-7.19 (3H, m, Ph), 7.04-7.06 (2H, m, Ph), 6.60 (2H, br, d, *J* = 4.8 Hz, Ph), 4.10-4.14 (1H, dd, *J* = 9.6, 4.4 Hz, CHC=O), 3.23 (1H, dd, *J* = 13.6, 4.4 Hz, Ph-CH_2), 3.15 (1H, dd, *J* = 13.6, 4.4 Hz, Ph-CH_2), 1.44 (9H, s, *t*-Bu) ppm; ^{13}C NMR (100 MHz, $CDCl_3$) δ: 171.1, 170.5, 139.9, 138.6, 136.7, 130.3, 130.1, 129.0, 128.5, 128.3, 128.3, 128.2, 127.9, 126.4, 81.3, 68.2, 46.5, 39.9, 28.3, 11.8 ppm. HPLC analysis: (Daicel Chiralcel OD-H), hexane/2-propanol = 100:1, flow rate = 1 mL/min, retention time: 14.9 min (R) and 39.7 min (S).

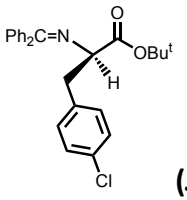

(*S*)-*tert*-butyl-N-(diphenylmethylene)-4-chlorophenylalaninate (3b): ^{1}H NMR (400 MHz, $CDCl_3$) δ: 7.57-7.59 (2H, m, Ar-H), 7.30-7.40 (6H, m, Ar-H), 7.16 (2H, d, *J* = 7.6 Hz, Ar-H), 7.00 (2H, d, *J* = 7.6 Hz, Ar-H), 6.69 (2H, br, d, *J* = 6.4 Hz, Ar-H), 4.10 (1H, dd, *J* = 8.8, 4.8 Hz, CHC=O), 3.10-3.22 (2H m, Ar-CH_2), 1.45 (9H, s, *t*-Bu) ppm; ^{13}C NMR (100 MHz, $CDCl_3$) δ: 170.9, 170.8, 139.7, 137.3, 136.6, 132.4, 131.5, 130.6, 129.1, 128.7, 128.5, 128.5, 128.3, 128.0, 81.6, 68.0, 39.3, 28.4 ppm. HPLC analysis: Daicel Chiralcel OD-H, hexane/2-propanol = 99:1, flow rate = 1 mL/min, retention time: 9.4 min (S) and 17.0 min (R).

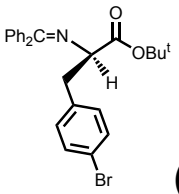

(*S*)-*tert*-butyl-N-(diphenylmethylene)-4-bromophenylalaninate (3c): ^{1}H NMR (400 MHz, $CDCl_3$) δ: 7.59 (2H, d, *J* = 7.6 Hz, Ar-H), 7.32-7.40 (8H, m, Ar-H), 6.95 (2H, d, *J* = 7.6 Hz, Ar-H), 6.69 (2H, br, d, *J* = 5.6 Hz, Ar-H), 4.10 (1H, dd, *J* = 8.8, 4.8 Hz, CHC=O), 3.09-3.20 (2H, m, Ar-CH_2), 1.45 (9H, s, *t*-Bu) ppm; ^{13}C NMR (100 MHz, $CDCl_3$) δ: 170.9, 139.7, 137.8, 136.6, 131.9, 131.4, 130.6, 129.0, 128.7, 128.5, 128.3, 127.9, 120.4, 81.6, 67.9, 39.3, 28.4 ppm. HPLC analysis: Daicel Chiralcel OD-H, hexane/2-propanol = 99:1, flow rate = 1 mL/min, retention time: 9.6 min (S) and 18.5 min (R).

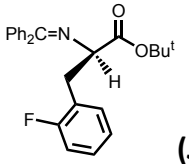

(*S*)-*tert*-butyl-N-(diphenylmethylene)-2-fluorophenylalaninate (3d): ^{1}H NMR (400 MHz, $CDCl_3$) δ: 7.58 (2H, d, *J* = 7.2 Hz, Ar-H), 7.28-7.38 (6H, m, Ar-H), 7.12-7.17 (2H, m, Ar-H), 6.89-6.99 (2H, m, Ar-H), 6.68 (2H, br, d, *J* = 6.8 Hz, Ar-H), 4.20 (1H, dd, *J* = 9.6, 4.4 Hz, CHC=O), 3.34 (1H, dd, *J* = 13.6, 4.4 Hz, Ar-CH_2), 3.16 (1H, dd, *J* = 13.6, 9.2 Hz, Ar-CH_2), 1.44 (9H, s, *t*-Bu) ppm; ^{13}C NMR (100 MHz, $CDCl_3$) δ: 170.9, 139.9, 136.6, 132.7, 132.7, 130.5, 129.1, 128.7, 128.4, 128.4, 128.3, 128.3, 128.0, 125.7, 125.6, 124.0, 123.9, 115.4, 115.2, 81.6, 66.5, 33.1, 28.4 ppm. HPLC analysis: Daicel Chiralcel OD-H, hexane/2-propanol = 99:1, flow rate = 1 mL/min, retention time: 11.7 min (R) and 21.2 min (S).

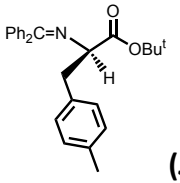

(*S*)-*tert*-butyl-N-(diphenylmethylene)-4-methylphenylalaninate (3e): ^{1}H NMR (400 MHz, $CDCl_3$) δ: 7.59 (2H, d, *J* = 7.2 Hz, Ar-H), 7.28-7.39 (6H, m, Ar-H), 7.00 (2H, d, *J* = 8.0 Hz, Ar-H), 6.95 (2H, d, *J* = 8.0 Hz, Ar-H), 6.64 (2H, br, d, *J* = 6.4 Hz, Ar-H), 4.10 (1H, dd, *J* = 9.2, 4.4 Hz, CHC=O), 3.21 (1H, dd, *J* = 13.6, 4.4 Hz, Ar-CH_2), 3.12 (1H, dd, *J* = 13.6, 9.2 Hz, Ar-CH_2), 2.29 (3H, s, CH_3), 1.45 (9H, s, *t*-Bu) ppm; ^{13}C

NMR (100 MHz, $CDCl_3$) δ: 171.3, 170.5, 140.0, 136.8, 135.9, 135.6, 130.4, 130.0, 129.1, 128.5, 128.4, 128.3, 128.1, 81.4, 68.4, 39.5, 28.4, 21.4 ppm. HPLC analysis: Daicel Chiralcel OD-H, hexane/2-propanol = 99:1, flow rate = 1 mL/min, retention time: 22.2 min (S) and 25.0 min (R).

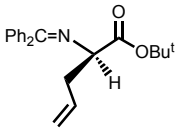

(*S*)-*tert*-butyl-2-[(diphenylmethylene)amino]pent-4-enoate (3f): ^{1}H NMR (400 MHz, $CDCl_3$) δ: 7.63-7.65 (2H, m, Ph), 7.30-7.47 (m, 6H, Ph), 7.16-7.19 (2H, m, Ph), 5.72 (1H, ddt, *J* = 17.2, 10.4, 7.2 Hz, C<u>H</u>=CH_2), 5.06 (1H, dd, *J* = 17.2, 1.6 Hz, *cis*-CH=C<u>H</u>$_2$), 5.01 (1H, dd, *J* = 10.4, 1.6 Hz, *trans*-CH=C<u>H</u>$_2$), 4.00 (1H, dd, *J* = 7.6, 5.6 Hz, CHC=O), 2.57-2.70 (2H, m, C<u>H</u>$_2$-CH=CH_2), 1.44 (9H, s, *t*-Bu) ppm; ^{13}C NMR (100 MHz, $CDCl_3$) δ: 171.2, 170.4, 140.1, 137.0, 135.1, 130.5, 129.1, 128.8, 128.7, 128.3, 128.3, 117.6, 81.4, 66.2, 38.5, 28.4 ppm. HPLC analysis: Daicel Chiralcel OD-H, hexane/2-propanol = 99:1, flow rate = 1 mL/min, retention time: 12.8 min (S) and 15.1 min (R).

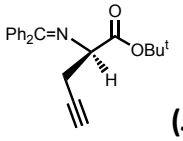

(*S*)-*tert*-butyl-2-[(diphenylmethylene)amino]pent-4-ynoate (3g): ^{1}H NMR (400 MHz, $CDCl_3$) δ: 7.65 (2H, d, *J* = 7.6 Hz, Ph), 7.31-7.45 (6H m, Ph), 7.25-7.27 (2H, m, Ph), 4.17 (1H, dd, *J* = 8.0, 5.6 Hz, CHC=O), 2.72-2.84 (2H, m, CH_2-C≡H), 1.95 (1H, t, *J* = 2.4 Hz, C≡H), 1.45 (9H, s, *t*-Bu) ppm; ^{13}C NMR (100 MHz, $CDCl_3$) δ: 171.7, 169.9, 140.0, 136.6, 132.7, 130.7, 130.4, 129.3, 129.0, 128.7, 128.6, 128.4, 82.0, 81.6, 70.4, 65.1, 28.4, 23.7 ppm. HPLC analysis: Daicel Chiralcel OD-H, hexane/2-propanol = 100:1, flow rate = 1 mL/min, retention time: 19.1 min (S) and 23.0 min (R).

Section 14. NMR Spectra of Catalytic Products

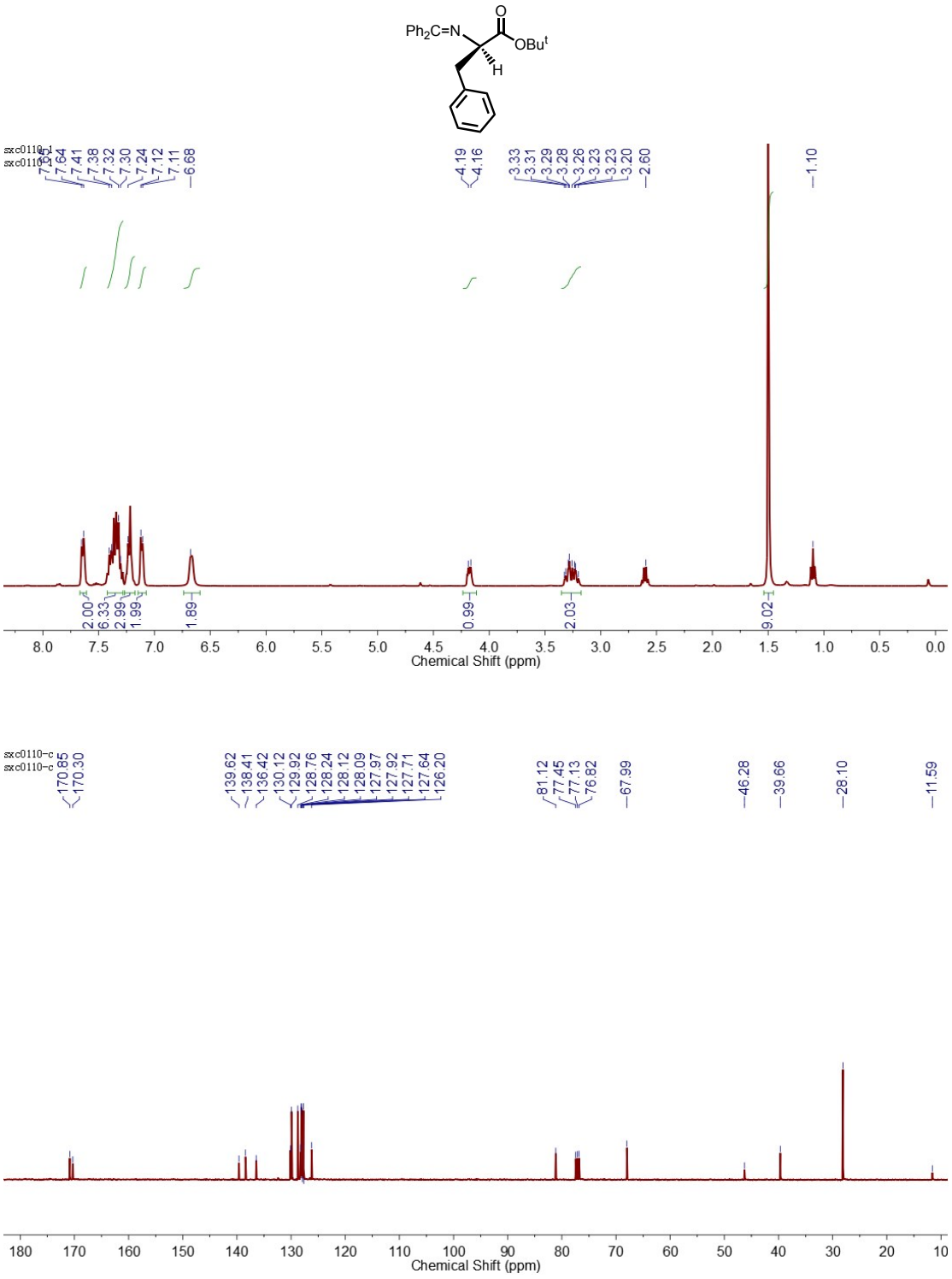

The ^{1}H-NMR and ^{13}C-NMR spectra of (*S*)-*tert*-butyl-N-(diphenylmethylene)phenylalaninate (3a).

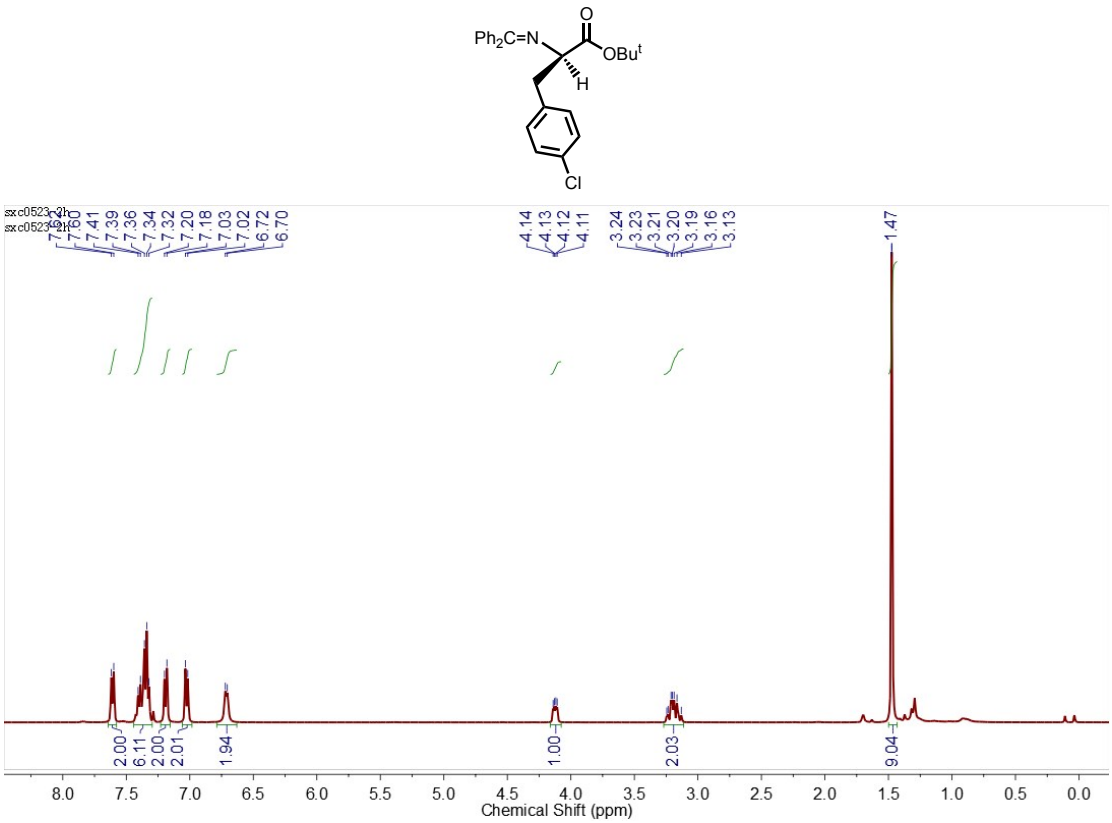

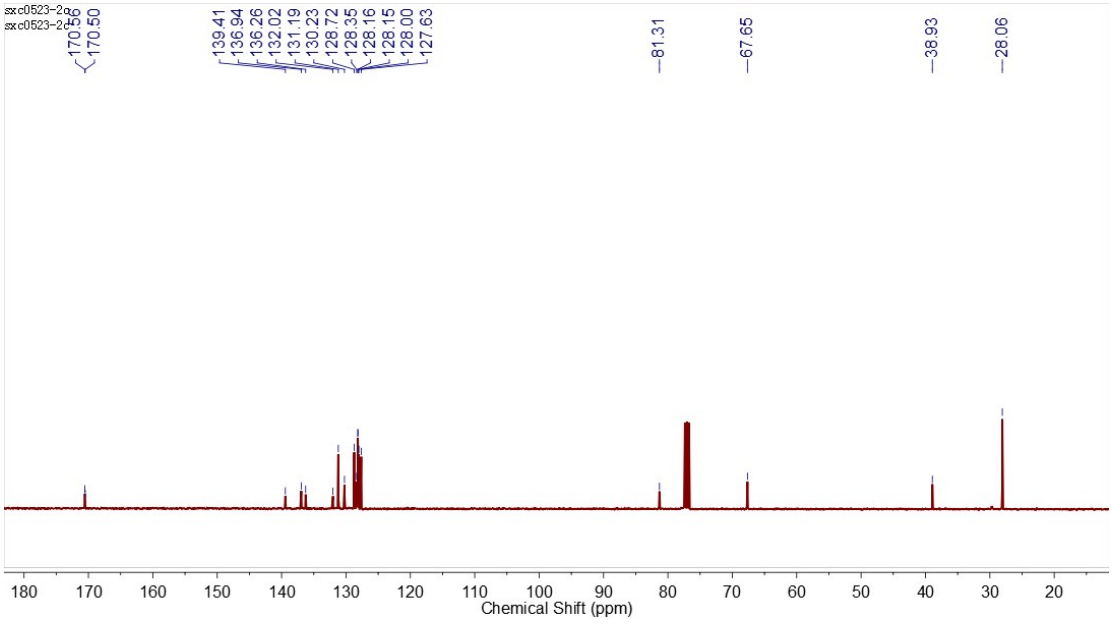

The ^{1}H-NMR and ^{13}C-NMR spectra of (*S*)-*tert*-butyl-N-(diphenylmethylene)-4-chlorophenylalaninate (3b)

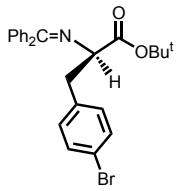

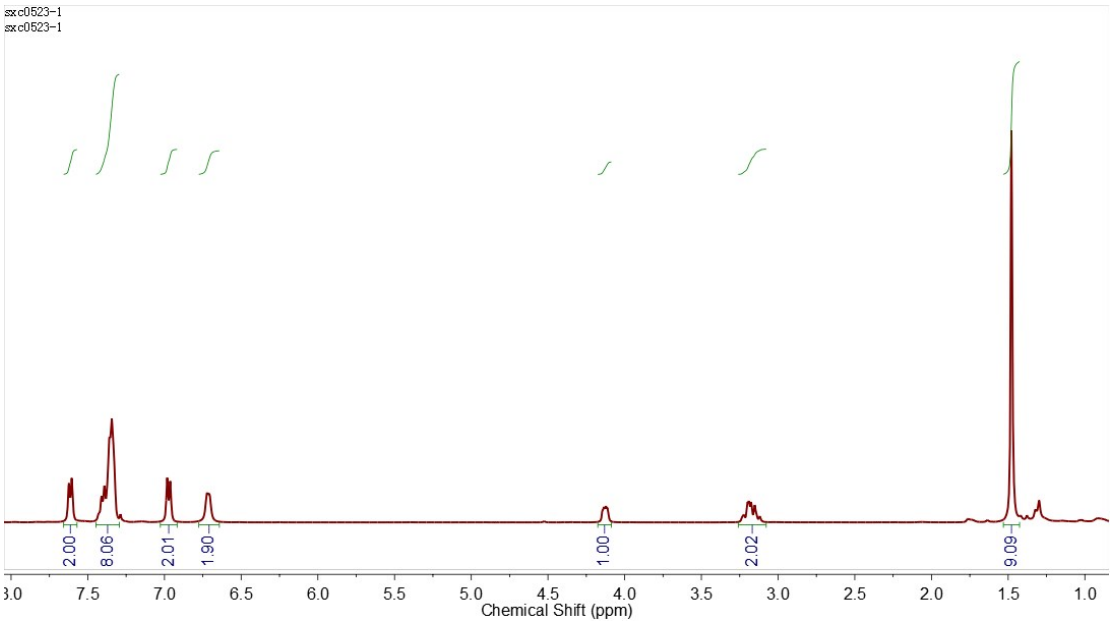

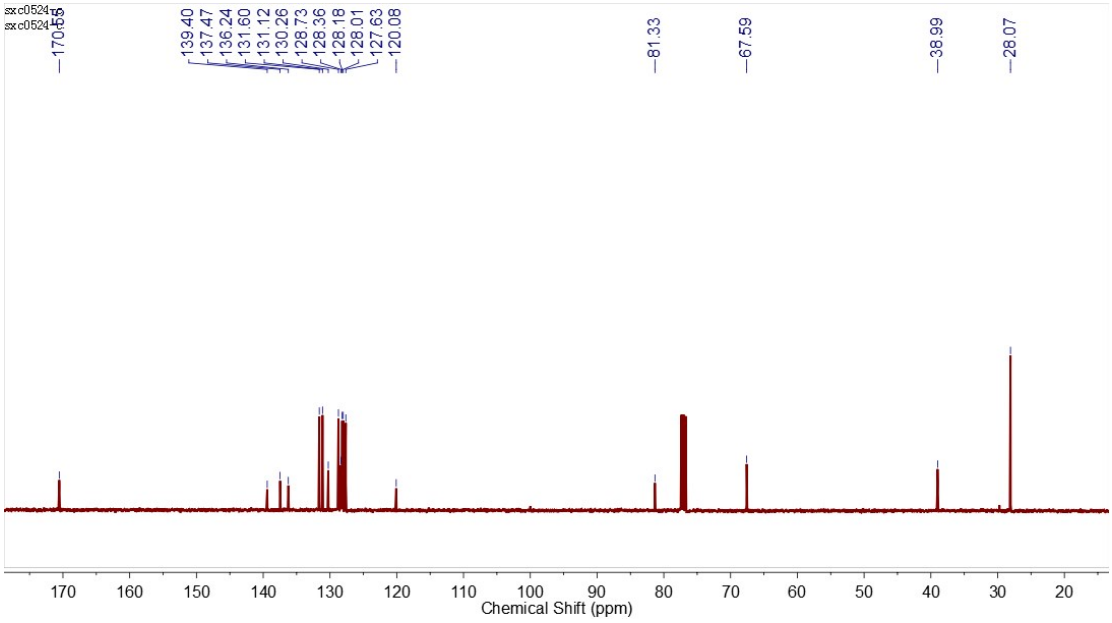

The ^{1}H-NMR and ^{13}C-NMR spectra of (*S*)-*tert*-butyl-N-(diphenylmethylene)-4-bromophenylalaninate (3c)

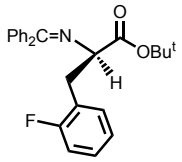

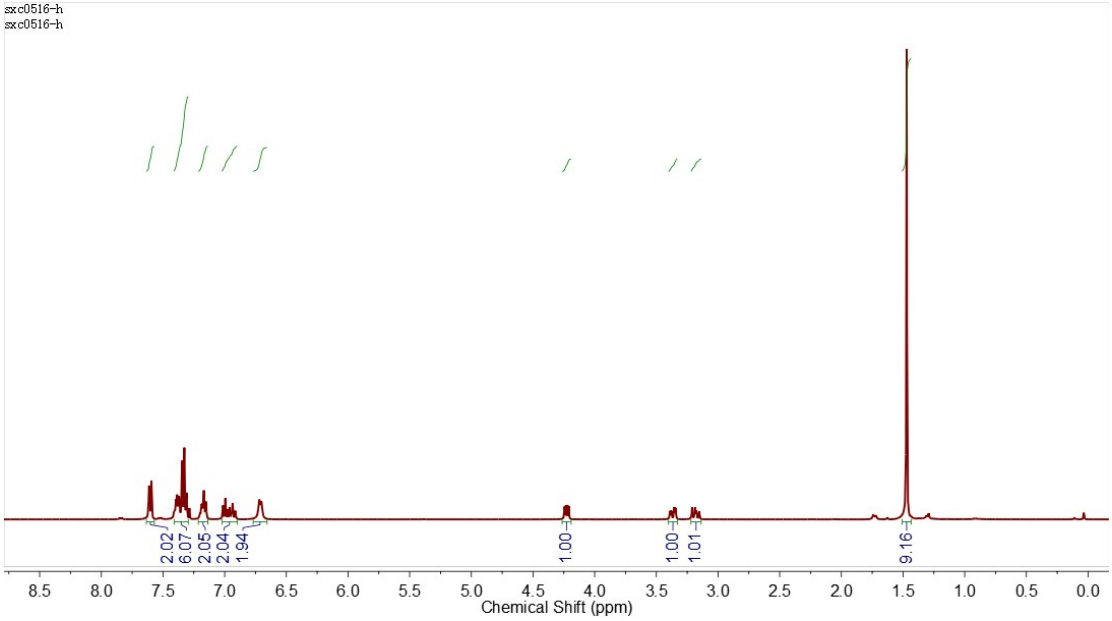

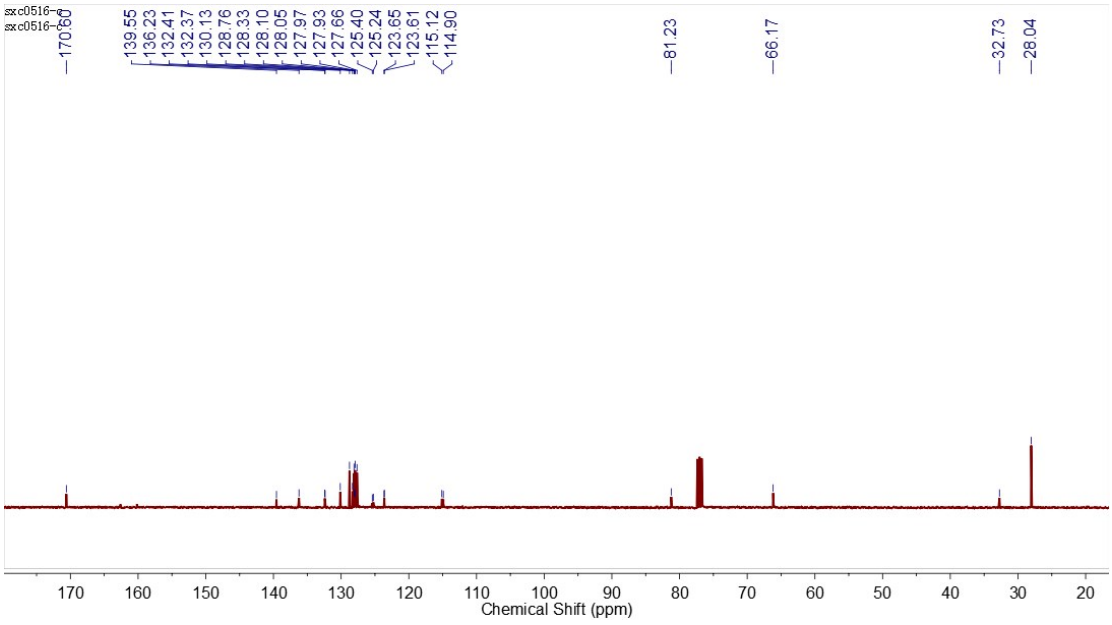

The ^{1}H-NMR and ^{13}C-NMR spectra of (*S*)-*tert*-butyl-N-(diphenylmethylene)-2-fluorophenylalaninate (3d)

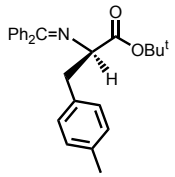

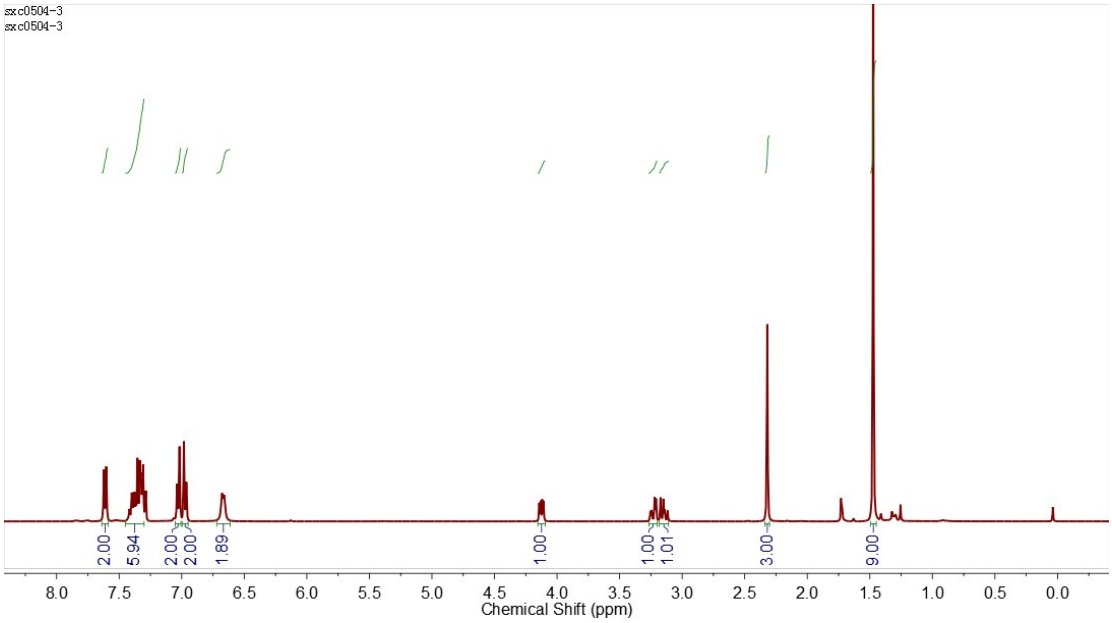

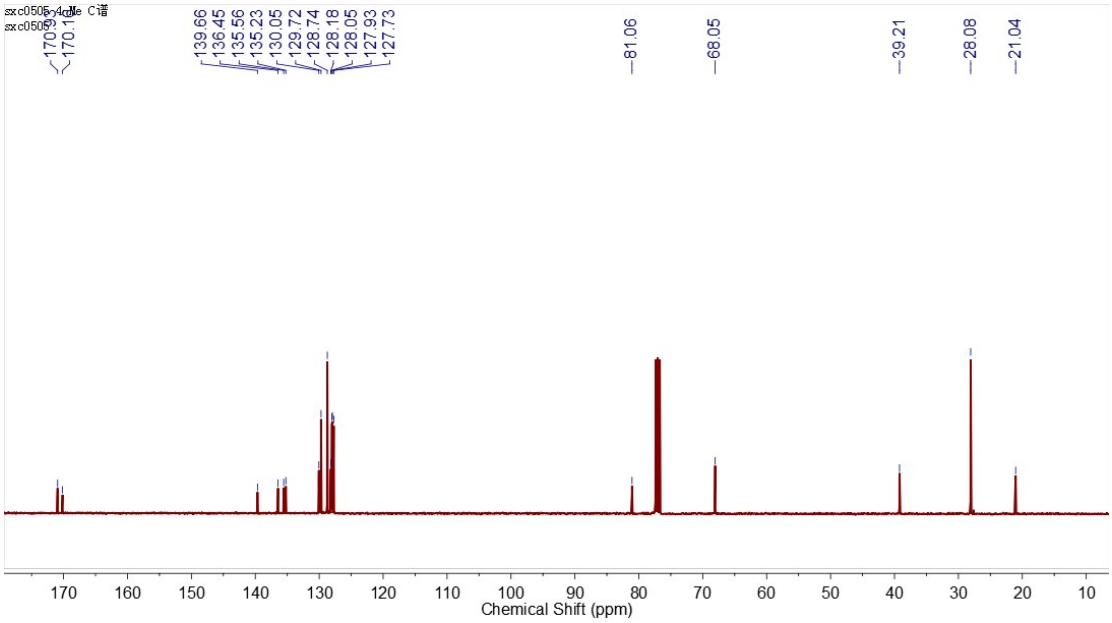

The ^{1}H-NMR and ^{13}C-NMR spectra of (*S*)-*tert*-butyl-N-(diphenylmethylene)-4-methylphenylalaninate (3e)

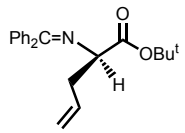

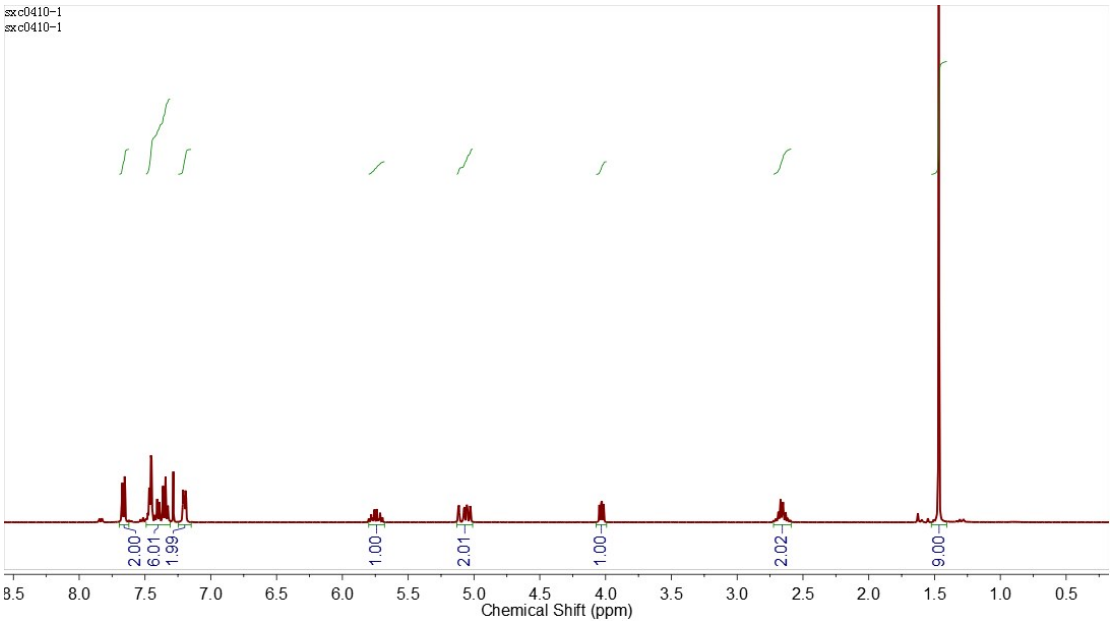

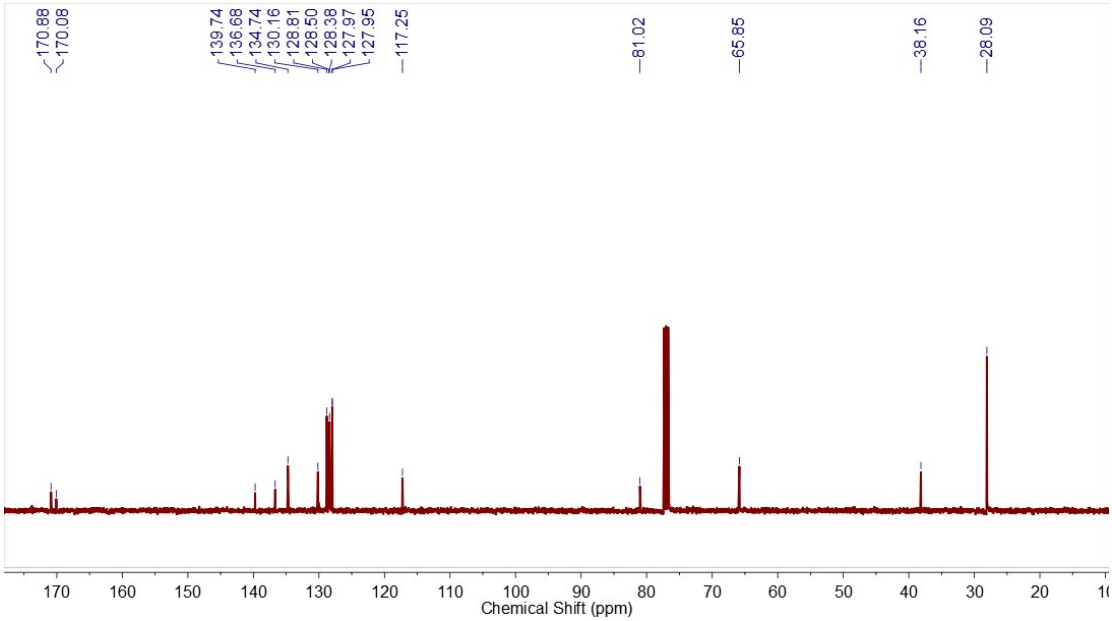

The ^{1}H-NMR and ^{13}C-NMR spectra of (*S*)-*tert*-butyl-2-[(diphenylmethylene)amino]pent-4-enoate (3f)

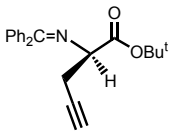

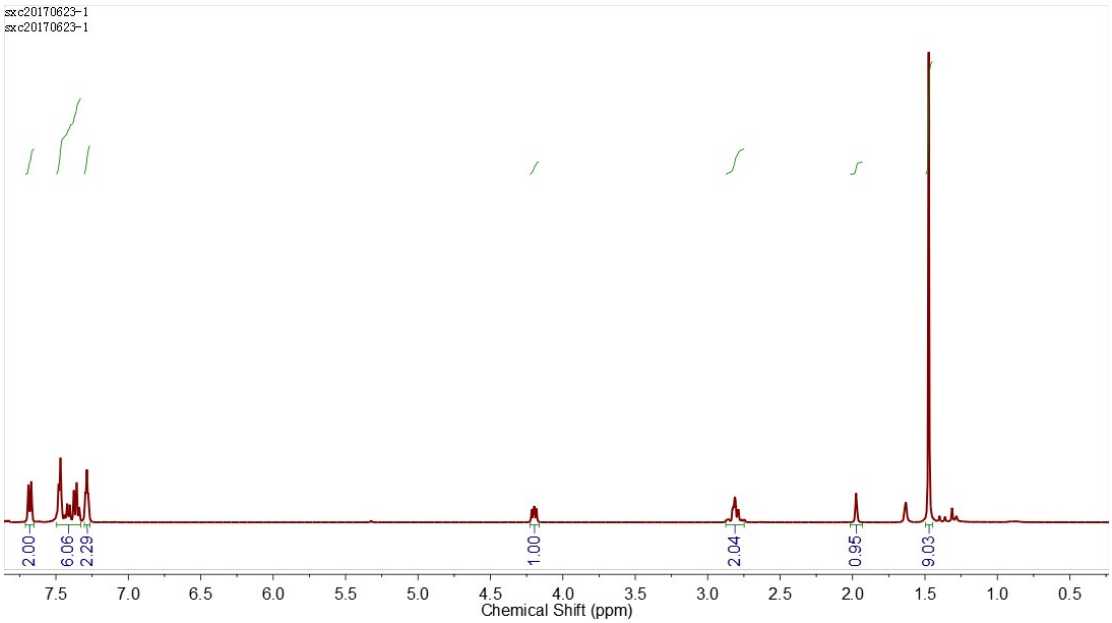

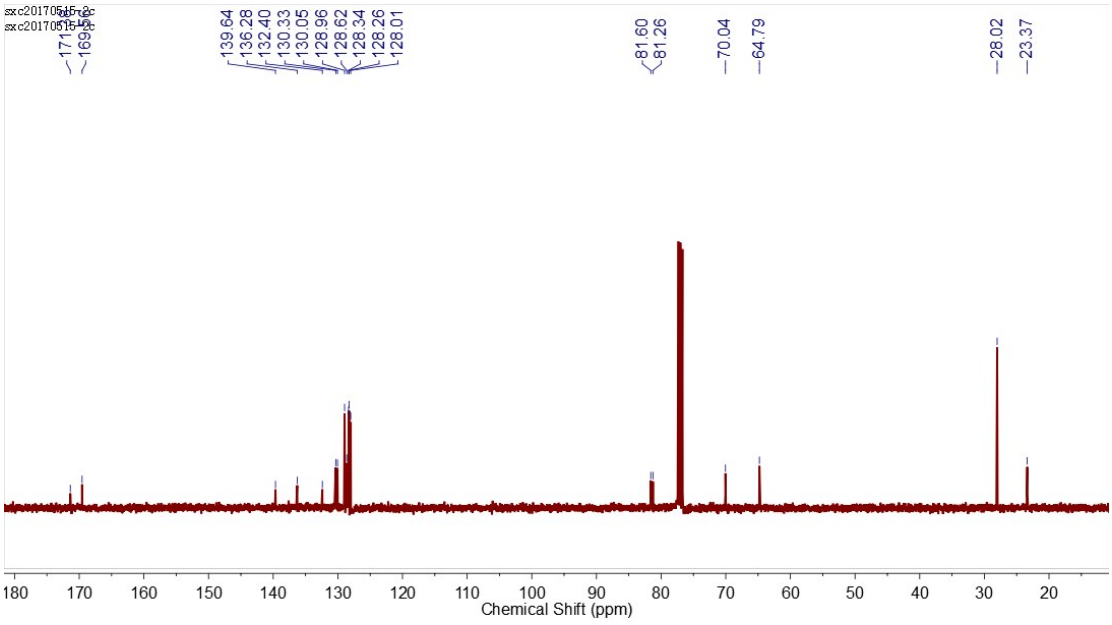

The ^{1}H-NMR and ^{13}C-NMR spectra of (*S*)-*tert*-butyl-2-[(diphenylmethylene)amino]pent-4-ynoate (3g)

Section 15. References

1. (*a*) X. Shen, S. Ma, H. Xia, Z. Shi, Y. Mu and X. Liu, *J. Mater. Chem. A*., 2018, **6**, 20653; (*b*) J. M. Hawkins, G. C. Fu, *J. Org. Chem.,* 1986, **51**, 2820; (*c*) T. Ooi, M. Kameda, K. Maruoka, *J. Am. Chem. Soc.,* 2003, **125**, 5139.